Copyright © 2000, by the author(s).
All rights reserved.

Permission to make digital or hard copies of all or part of this work for personal or classroom use is granted without fee provided that copies are not made or distributed for profit or commercial advantage and that copies bear this notice and the full citation on the first page. To copy otherwise, to republish, to post on servers or to redistribute to lists, requires prior specific permission.

MODELING FIELD ENHANCEMENT IN AN RF GAP

by

E. Kawamura, J. P. Verboncoeur and C. K. Birdsall

Memorandum No. UCB/ERL M00/22

18 May 2000

MODELING FIELD ENHANCEMENT IN AN RF GAP

by

E. Kawamura, J. P. Verboncoeur and C. K. Birdsall

Memorandum No. UCB/ERL M00/22

18 May 2000

ELECTRONICS RESEARCH LABORATORY

College of Engineering
University of California, Berkeley
94720

Modeling field enhancement in an rf gap

E. Kawamura, J. P. Verboncoeur, C. K. Birdsall

EECS Dept., 195M Cory Hall

University of California at Berkeley

Berkeley, CA 94720-1770

1 Introduction

The high electric fields applied to microwave cavities induce field emission of electrons. This field emission current I_{FE} combined with neutral desorption at the nose cones of a microwave cavity can lead to surface damage. The field emission current heats the metal surfaces, leading to desorption of neutral contaminants on the surfaces. The field emitted electrons ionize the desorbing neutrals. The resulting positive ions enhance the field at the emitter, increasing I_{FE}. The higher I_{FE} increases the power dissipation and the temperature of the emitter, leading to more neutral desorption. More neutrals imply more positive ion creation and field enhancement, etc., leading to positive feedback loop. Eventually, the emitter surface will melt and is ``rf processed". Figure 1a shows the cross-section of a microwave X- band cavity, and Fig. 1b shows the damage on one of its nose cones [1].

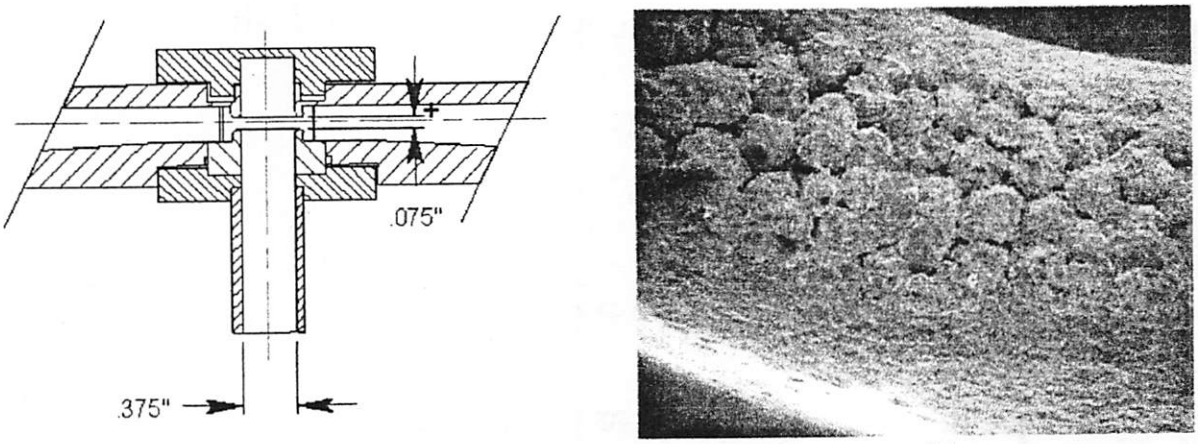

(a) (b)

Figure 1: (a) Cross-section of the first X-band cavity. (b) Portion of the rim of the cavity nose that has the most damage. Magnification is 50x. From reference [1].

We use a 1d3v particle-in-cell/Monte-Carlo collisions (PIC/MCC) model to show the effect of positive space charge on I_{FE}. The model consists of two parallel plates; the left plate is driven by a sinusoidal rf voltage source and the right plate is grounded. I_{FE} is given by the Fowler-Nordheim relation. Our first model assumes a constant and uniform neutral background while a second model takes neutral flows and gradients into effect. In both models, we observed field enhancement due to positive ion formation. We assume that hydrogen atoms desorb from the copper surfaces of the cavity. The 1d3v PIC/MCC simulation code PDP1 self-consistently solves for the fields due to the applied rf and the charges [2].

1.1 Field emission

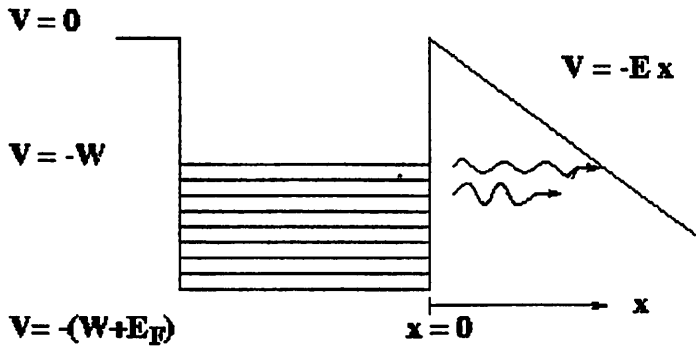

Figure 2: e's may tunnel through the potential barrier, especially where the barrier is thinner.

Electrons may be extracted from conductors by applying a strong electric field. Applying a high field to the metal produces a triangular potential barrier through which electrons at the metal surface may tunnel quantum mechanically, especially where the tunnel is thinner. (See Fig. 2). By solving Schrodinger's equation, Fowler and Nordheim obtained the barrier penetration probability D(ε), where ε is the kinetic energy of the electrons in the metal. By multiplying D(ε) by the number of electrons arriving at the surface with kinetic energy ε and integrating over all ε, Fowler and Nordheim derived the ``Fowler-Nordheim" equation relating field emission current density j_{FE} (A/m^2) with emitter electric field E (V/m) and work function W (eV) [3].

$$j_{FE} = \frac{1.54\times10^{-6}\times10^{4.52W^{-1/2}}E^2}{W}\exp(-\frac{6.53\times10^{9}W^{3/2}}{E}), \qquad (1)$$

Typically, field emission occurs at fields of the order of 10^9 - 10^{10} V/m.

Fowler and Nordheim calculated the current for a cold flat surface. The current is weakly dependent on temperature, but it is strongly dependent on emitter shape. To take shape into account, there is a geometric field enhancement parameter $\beta = E/E_{applied}$, the ratio of the local emitter field over the applied field. Plugging this into Eq. (1), we obtain

$$j_{FE} = \frac{1.54\times10^{-6}\times10^{4.52W^{-1/2}}(\beta E_{applied})^2}{W}\exp(-\frac{6.53\times10^{9}W^{3/2}}{\beta E_{applied}}), \qquad (2)$$

2 Field enhancement

The following flow chart (Fig. 3) illustrates the positive feedback loop that may lead to `rf processing" of the emitter. The field emission of electrons heats the metal emitter, leading to desorption of neutral contaminants. The electrons collide with the neutrals and create positively charged ions near the emitter. The ions neutralize the self-field of the emitted electrons and also enhance the electric field, creating larger field emission currents I_{FE}. Ions also provide a dc bias so that the fraction of the rf cycle during which field emission is active increases, leading to larger average field emission currents. Power dissipation at the emitter will increase with increasing emission current. This will increase the temperature of the emitting surface, leading to more neutral desorption. This increase in neutral flux will increase the ionization rate which will increase the emission current, and so on, causing a positive feedback loop. At some point the emitter temperature will reach its melting point and the emitter surface is ``rf processed" [4].

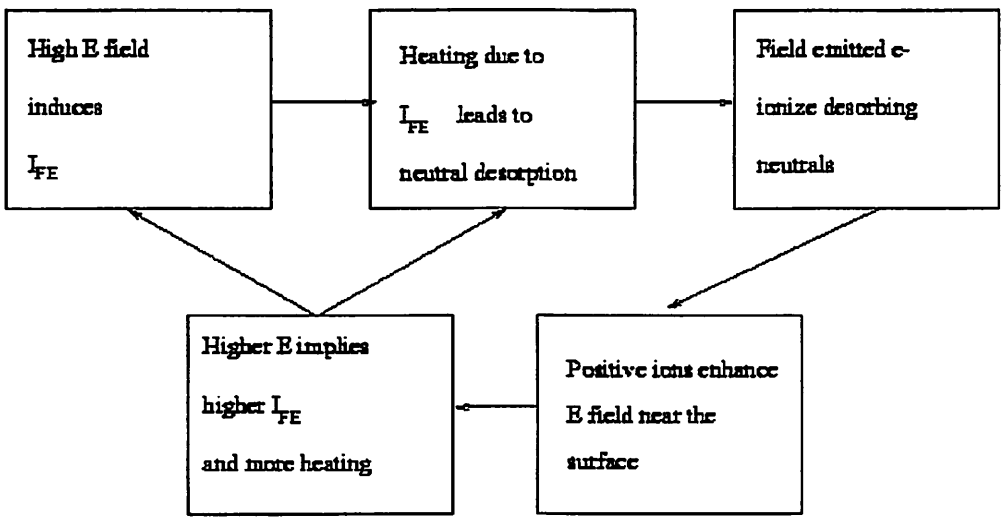

Figure 3: Positive feedback loop leading to "rf processing" or melting of the emitter surface.

3 RF gap simulation model

We modeled the nose cones of the microwave cavity with two parallel plates of diameter 5 mm and spacing of 2 mm. The initial applied field was 120 MV/m and the applied frequency was 11.424 GHz. We assumed that the gap was filled with atomic hydrogen. Though pressure within the entire cavity is low (~10^{-8} Torr), the neutral pressure may be high near the surface of the emitter when neutrals desorb from the surface.

We are mainly interested in the region near the field emitter. At 120 MV/m, the electron energy is already 1200 eV after 10 μms. The electron impact ionization cross section peaks at about 100 eV and then starts to decline. Also, we get significant neutral density only near the emitter where the neutral desorption occurs. Thus, most of the ionizations occur within a few μms of the emitter. Thus, we limited our simulation to a 10 μm region near the emitter.

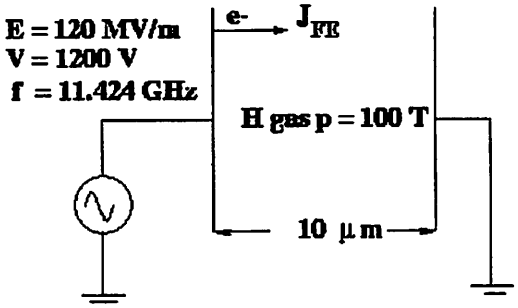

Figure 4: RF gap simulation model near emitter region.

Since the electrons reach maximum energies of about 1200 eV, corresponding to velocities of about 0.05 c, we neglected relativistic effects and the self magnetic field of the electrons, and used an electrostatic field solve. To avoid having electrons move more than one cell per timestep, and to resolve submicron distances, we used femtosecond (10^{-15} sec.) timesteps.

The Fowler-Nordheim current density is given by,

$$\begin{aligned} j_{FE} &= AE_{applied}^2 \exp(-B/|E_{applied}|), \quad for \quad E_{applied} < 0 \\ &= 0, \quad for \quad E_{applied} > 0 \end{aligned} \tag{3}$$

where $E_{applied}$ is the instantaneous electric field at the emitter site, and A and B are input parameters supplied by the user and which depend on the work function W and geometric enhancement factor β of the emitter. We assumed that the metal was copper with $W = 4.59$ eV. We also assumed a β of 50. (See Fig. 3 of Reference [3]). The electrons emitted from the surface were assumed to have a temperature of 500 C. Furthermore, the electron drift velocity normal to the surface was randomly chosen from the range 0.1 V to 1V.

Our collision model was the standard Monte Carlo collisions (MCC) package [5]. We included only electron-hydrogen atom collisions for ionization, excitation and elastic scattering. This may be improved by allowing more types of collisions in the future. However, the main

reaction of interest is the ion production from ionization.

We also assume that enough neutrals have desorbed in the region near the emitter surface to produce a high neutral pressure of about 100 Torr. As a first approximation, we assume a constant uniform neutral pressure in this 10 μm region. A monolayer of hydrogen atoms has a surface density of about 1.5×10^{19} atoms/m^2. (See for example Table 2.17 of reference [6].)
A suddenly released monolayer will form a dense expanding gas in the 10 μm region of approximate density, $n_g = 1.5\times10^{19}$ atoms/m^2 ÷ 10 μm = 1.5×10^{24} m^{-3}. The emitter surface has an initial temperature of about T=500 C=737 K. Thus, the pressure in the cavity is approximately, $p = n_g k_B T \approx 1.5\times10^{24}$ m^{-3} × 1.38×10^{-23} J/K × 737 K ≈ 1.5×10^{4} Pa ≈ 100 Torr.

4 Simulations with constant and uniform neutral background

We used the rf gap model described above to do some PIC/MCC simulations. The simulations were conducted for several rf cycles. We did two cases.

- Case 1: Collisions are turned off so that there are no ions created in the gap. There is no field enhancement at the emitter.
- Case 2: Collisions are turned on so that ions are created near the emitter. The positive ions enhance the field at the emitter. The ions also produce a positive dc bias so that the fraction of the rf cycle in which the field emission is turned on ($E < 0$) increases. (See Fig. 5).

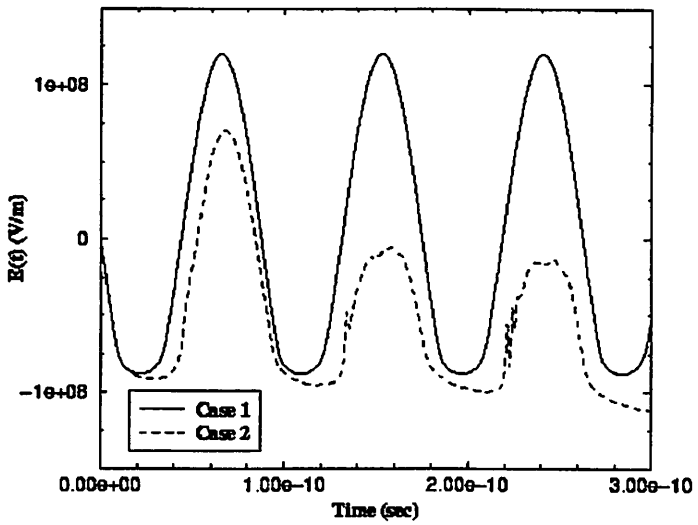

Figure 5: Electric field at emitter vs. time for cases 1 and 2. A constant and uniform neutral background is assumed for this set of simulations.

5 Simulations with neutral flow and gradient

We improved our PIC/MCC model by incorporating a time varying neutral flow. At t=0, a monolayer of 1.5×10^{19} H atoms/m^3 is released from the emitter. The emitted neutrals are assumed to have a Maxwellian velocity distribution with temperature T_g = 500 C = 737K. As in the previous section, we conducted two cases. In case 1, the collisions are turned off so that no ions are created in the gap. In case 2, the collisions are turned off so that ions are created near the emitter. As with the previous simulations, the ions enhance the field at the emitter and generate a dc bias so that the fraction of the rf cycle during which field emission is turned on increases. However, it takes a couple of rf cycles for the field enhancement to begin because the neutral atoms need time to flow into regions in which the electrons have reached ionization energies (> 13.6 eV). (See Fig. 6).

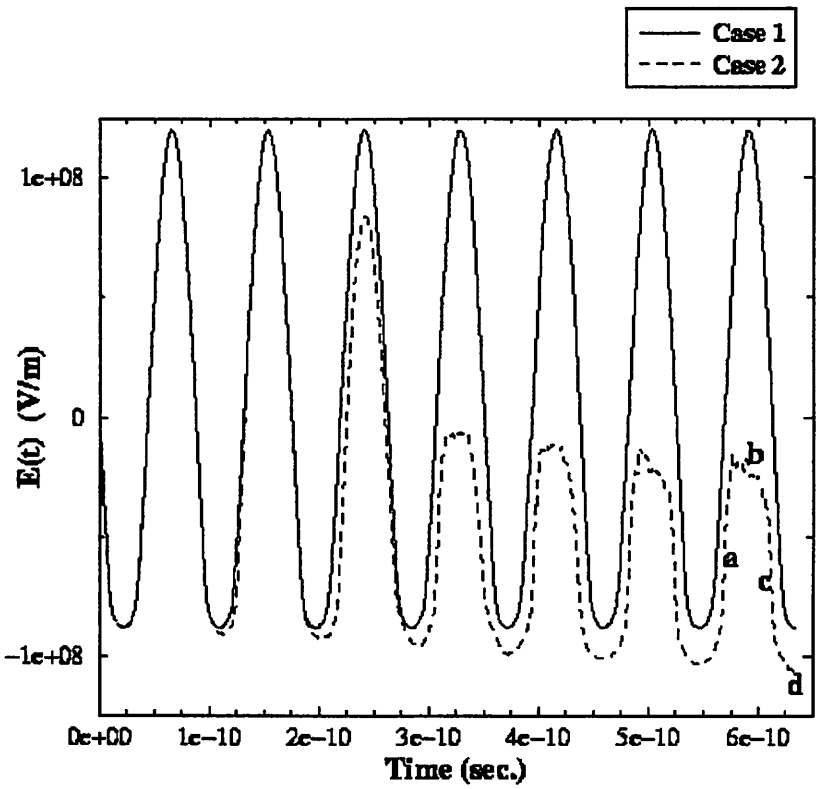

Figure 6: Electric field at emitter vs. time for cases 1 and 2. A time-varying neutral flow is incorporated into this set of simulations by assuming that a monolayer of H atoms is released from the emitter at time t = 0. Points **a**, **b**, **c**, and **d** on the plot correspond to t = 6.5, 6.75, 7, and 7.25 rf cycles respectively.

Points **a**, **b**, **c**, and **d** in Fig. 6 correspond to t = 6.5 rf cycles, 6.75 rf cycles, 7 rf cycles, and 7.25 rf cycles respectively. The following diagnostics (Figures 7-10) show the densities, electric fields, and potentials for cases 1 and 2 at these times.

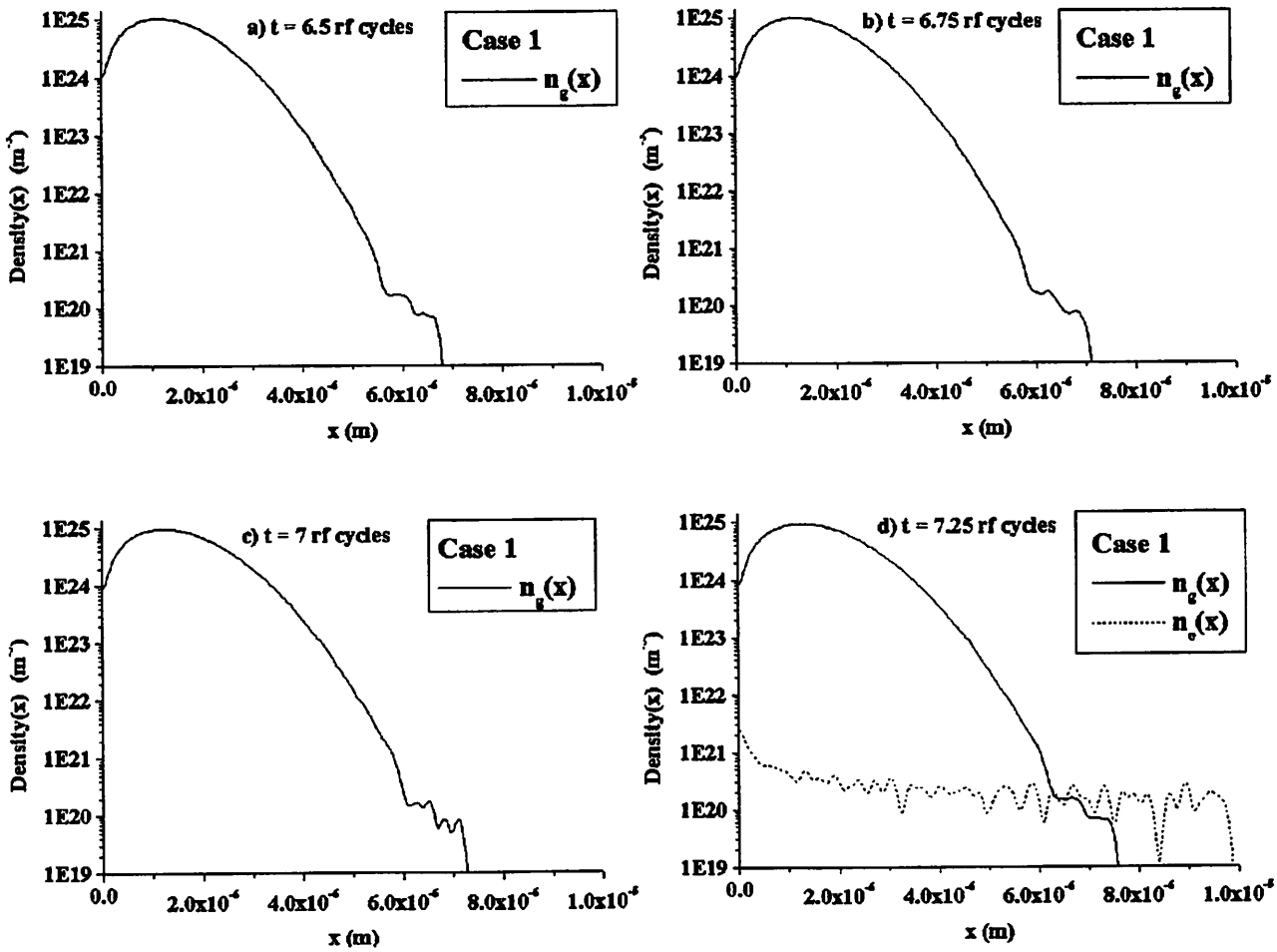

Figure 7: Case 1 densities at t = 6.5, 6.75, 7, and 7.25 rf cycles.

Let us compare the time evolution of the gas density $n_g(x)$, electron density $n_e(x)$ and ion density $n_i(x)$ for cases 1 and 2 (Fig. 7 and 8). For case 1, there is no positive ion formation since collisions are turned off. Also, field emission is turned on only for the last ¼ cycle (point **d**) when the field is at its most negative values. For case 2, an electron-ion pair is created for every electron-impact ionization. This increases the electron density and generates ions. Field emission is active over a greater fraction of the rf cycle than in case 1. Also, the field enhancement due to the ions also increases the field emission and leads to greater electron densities.

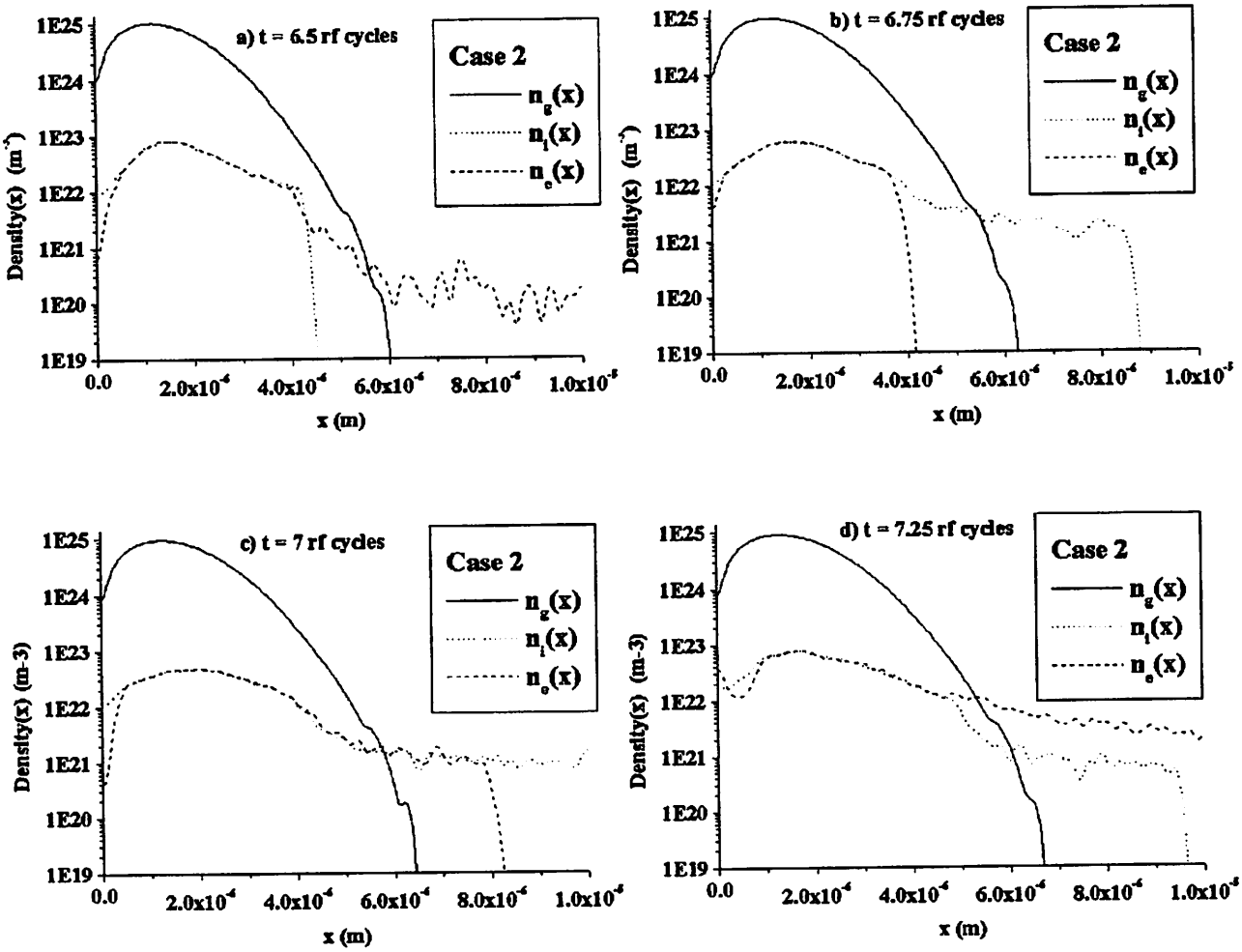

Figure 8: Case 2 densities at t = 6.5, 6.75, 7, and 7.25 rf cycles.

The enhancement of the field due to the positive ion formation can also be observed in Figures 9 and 10 which compare the fields and potentials of cases 1 and 2 respectively. We know from Eq.'s (1) and (2) that the more negative $E(x)$ is at the emitter (x = 0), the higher the field emission. Figure 9 clearly shows the field enhancement in case 2. In Fig. 10, for case 2, the slope of the potential $V(x)$ is greater than or equal to zero at the emitter. Thus, for case 2, the slope of an electron's potential energy curve $U(x) = -eV(x)$ is less than or equal to zero at the emitter, and the electron will tend to fall down a potential hill, enhancing field emission. This increased field emission from the field enhancement leads to the positive feedback loop described above.

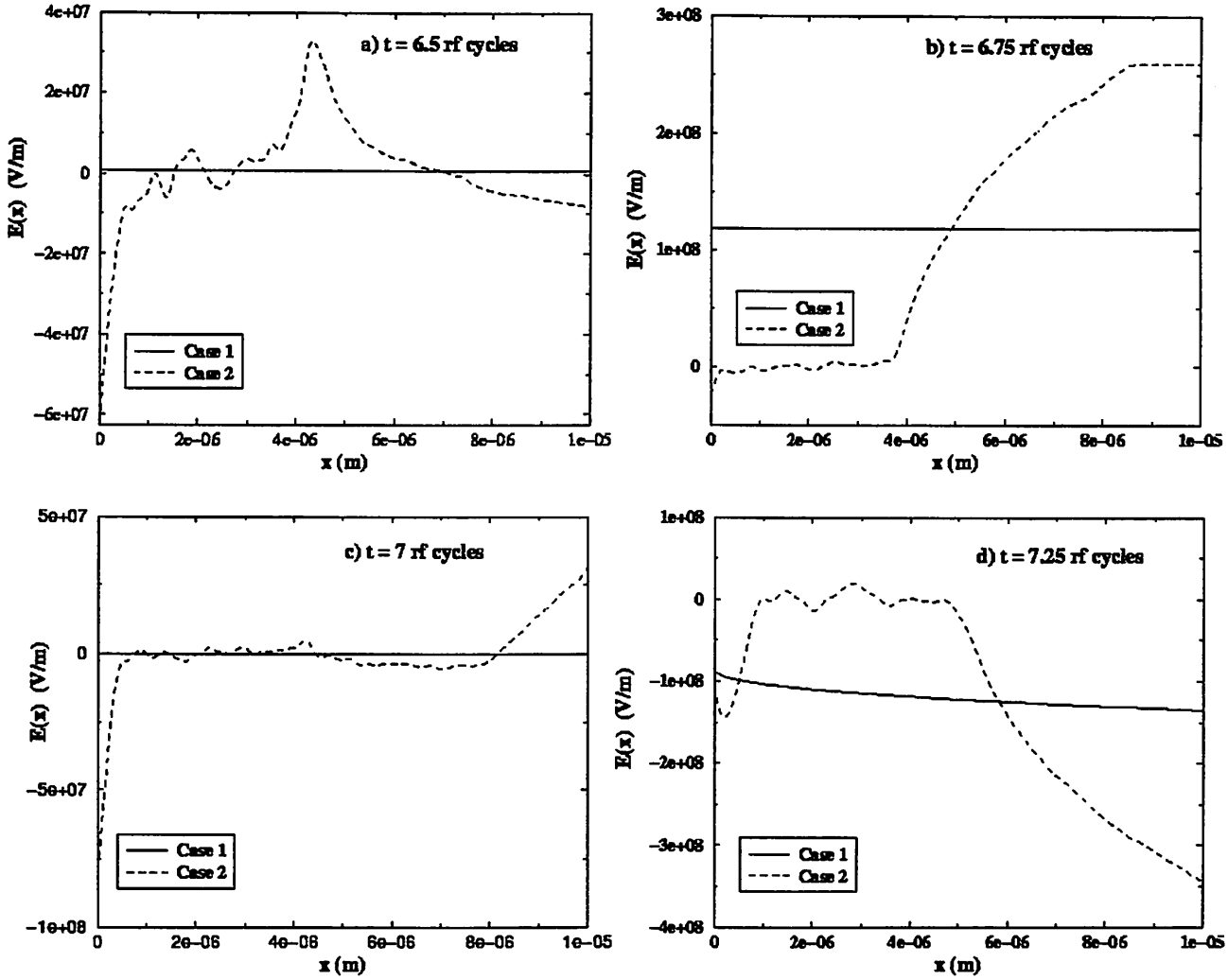

Figure 9: Electric field *E(x)* for case 1 (solid line) and case 2 (dashed line) at times t = 6.5, 6.75, 7, and 7.25 rf cycles. Note the field enhancement at the emitter ($x = 0$) in case 2.

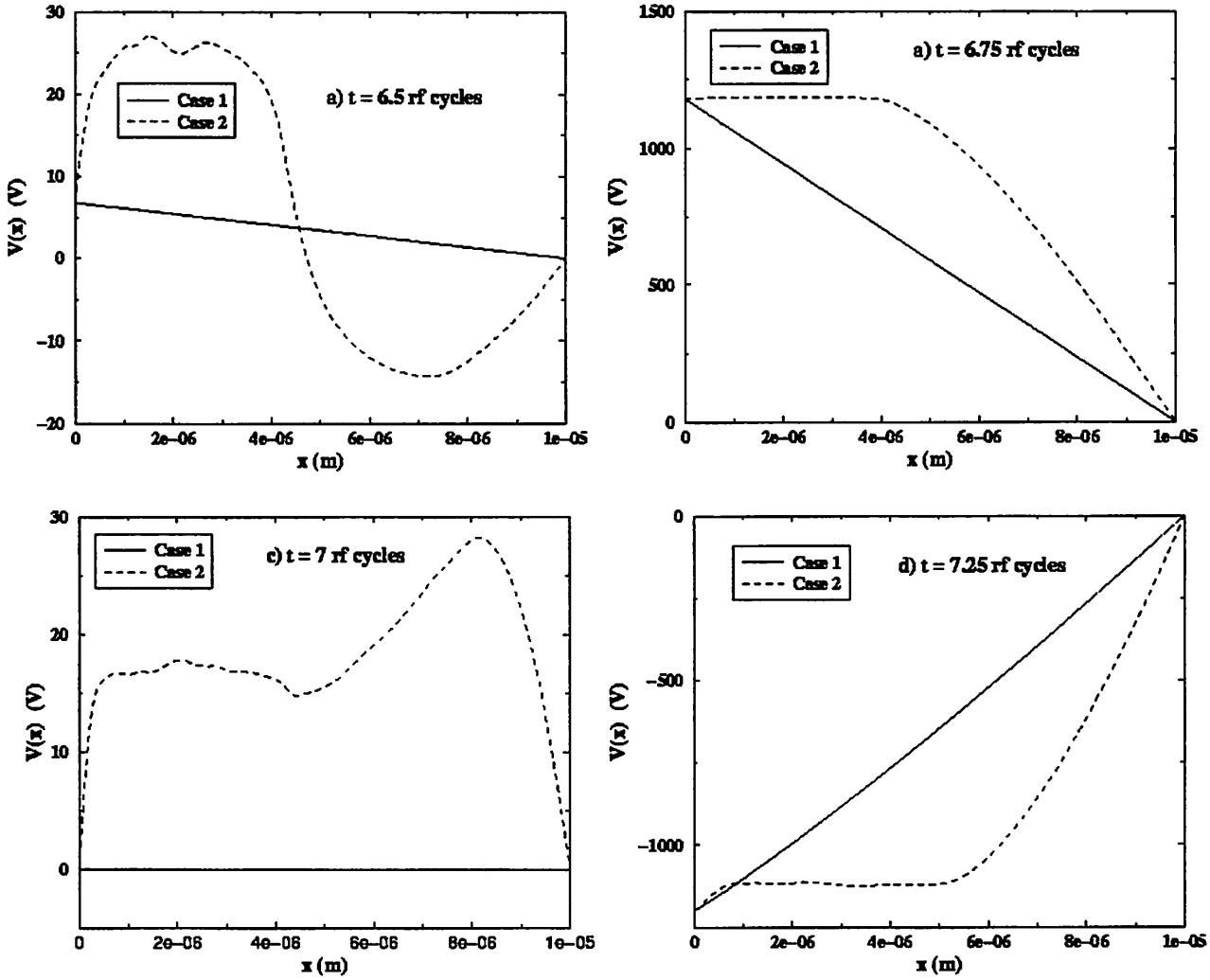

Figure 10: Potential *V(x)* for case 1 (solid line) and case 2 (dashed line) at times t = 6.5, 6.75, 7, and 7.25 rf cycles.

6 Improved neutral flow model

So far our neutral flow model consists of a suddenly released monolayer of gas atoms. However, the actual desorption of neutrals from the surface would be more complicated. We can attempt to model this desorption in two steps. First, we must determine the emitter temperature as a function of time due to heating from the field emission current. Then, we must determine the desorption of atomic H from a copper emitter as a function of the emitter temperature.

To determine the temperature of the emitter, we may model it as a one-dimensional semi-infinite slab. Then, from the heat equation, we have,

$$\frac{\partial^2 T(x,t)}{\partial x^2} - \frac{\rho c_v}{K}\frac{\partial T(x,t)}{\partial t} = -\frac{Q(x,t)}{K}. \qquad (4)$$

where $T(x,t)$ is the absolute temperature, $Q(x,t)$ is the heat source (in our case, the Joule heating from the field emission current), K is the thermal conductivity, c_v is the heat capacity, and ρ is the density of the material. All the coefficients in the heat equation depend on T so that the equation is non-linear. However, for simplicity, we can use a linearized equation in which the coefficients are evaluated at some $T=T_0$.

The boundary and initial conditions for the semi-infinite cathode are as follows:
(i) The initial temperature is T_0, or $T(x,0) = T_0$. (ii) No temperature rise is experienced at the far end of the medium so that $T(\infty, t) = T_0$. (iii) The temperature gradient at the interface matches that resulting from the heat source, or $\partial T(0,t)/\partial x = -(1/K)\,\partial Q(0,t)/\partial x$.

Let us assume that the H atoms are physisorbed on the Cu surface. To determine the rate of desorption of α neutrals/m^2 from a homogeneous surface in the event that none is returning from the gas phase, we may assume first order desorption [6]:

$$\frac{d\alpha}{dt} = -\frac{\alpha k_B T}{h}\exp\left(-\frac{E_d}{k_B T}\right) \qquad (5)$$

where E_d is the activation energy for desorption, k_B is the Boltzmann constant, and h is the Planck constant.

Once we have incorporated the neutral flow into our model, we can further refine the model by including the effects of ion bombardment on the emitter. We expect the ion bombardment to further heat the surface and lead to further neutral desorption.

7 Empirical data

Many of the parameters needed to model field enhancement depends exactly on how the cavity was prepared. For example,

- Were the metal surfaces of the chamber polished. If so, how?
- Were the chamber walls baked during pump down? If so, what was the temperature duration of the bake out?

The hydrogen concentration in the copper and the hydrogen outgassing rate will depend crucially on this history.

The surface conditons also influence the field emission of electrons. For example:

- Surface defects and grain boundaries may alter the work function of the metal and affect field emission rate. They may also affect the hydrogen outgassing rate.
- Without a better understanding of the geometric field enhancement factor β, a quantitative analysis of field enhancement would be difficult.

Time resolved data would be useful in testing any model. Examples of such data would be

- The temperature of an emitter surface vs. time
- The surface coverage of H atoms on Cu vs. time
- The current vs. time
- The outgassing rate of hydrogen atoms vs. time
- The ion bombardment rate vs. time.
- The electron, ion, neutral densities in the cavity vs. time.

It is advisable to gather more detailed empirical data on the field enhancement problem before embarking on a full-scale model.

8 Conclusion

By using particle simulations, we demonstrated that large positive ion densities can develop near an emitter when field emitted electrons collide with desorbing neutrals. We also showed that the positive ions enhance the field at the emitter. In our first model, we used a constant and uniform neutral background. Then, we incorporated neutral flow into our model by assuming that a monolayer of atoms was released from the emitter surface at the start of the simulation. In order to use more sophisticated neutral desorption models, we need a better understanding of the emitter surface physics. This may be gained by gathering time-resolved empirical data such as the outgassing rate, ion bombardment rate, temperature, densities, and surface coverage at the emitter.

Acknowledgments

We are grateful to AFOSR/MURI contract F49620-95-1-0253, and we would also like to thank Glenn Scheitrum and Lisa Laurent at SLAC.

References

[1] The images may be downloaded from the website http://www.slac.stanford.edu/grp/kly/

[2] J. P. Verboncoeur, M. V. Alves, V. Vahedi, and C. K. Birdsall, "Simultaneous Potential and Circuit Solution for 1d Bounded Plasma Particle Simulation Codes", *J. Comput. Phys.*, **104**:321-328 (1993).

[3] J. W. Wang and G. A. Loew, "Field Emission and RF Breakdown in High-Gradient Room-Temperature Linac Structures", SLAC center, Stanford University, not yet published.

[4] J. Knobloch, ``Advanced Thermometry Studies of Superconducting RF Cavities", Ph. D. Thesis, Cornell University, (1997).

[5] V. Vahedi and M. Surendra, "Monte-Carlo Collision Model for Particle-in-Cell Method: Application to Argon and Oxygen Discharges", *Comp. Phys. Comm.*, **87**:179-198 (1995).

[6] P. A. Redhead, J. P. Hobson, and E. V. Kornelsen, ``The Physical Basis of Ultrahigh Vacuum", Chapman and Hall Ltd., (1968).